4036 *Biochemistry* **2010,** *49,* 4036–4042
DOI: 10.1021/bi1001568

BIOCHEMISTRY
including biophysical chemistry & molecular biology
Article

Interactions of Coenzyme A with the Aminoglycoside Acetyltransferase (3)-IIIb and Thermodynamics of a Ternary System[†]

Adrianne L. Norris[‡] and Engin H. Serpersu*[,‡,§]

[‡]*Department of Biochemistry and Cellular and Molecular Biology, The University of Tennessee, Knoxville, Tennessee 37996, and* [§]*Graduate School of Genome Science and Technology, The University of Tennessee and Oak Ridge National Laboratories, Knoxville, Tennessee 37996, and Bioscience Division, Oak Ridge National Laboratory, Oak Ridge, Tennessee 37831*

Received February 1, 2010; Revised Manuscript Received April 9, 2010

ABSTRACT: In this work, the binding of coenzyme A (CoASH) to the aminoglycoside acetyltransferase (3)-IIIb (AAC) is studied by several experimental techniques. These data represent the first thermodynamic and kinetic characterization of interaction of a cofactor with an enzyme that modifies the 2-deoxystreptamine ring (2-DOS) common to all aminoglycoside antibiotics. Acetyl coenzyme A (AcCoA) was the preferred substrate, but propionyl and malonyl CoA were also substrates. CoASH associates with two different sites on AAC as confirmed by ITC, NMR, and fluorescence experiments: one with a high-affinity, catalytic site and a secondary, low-affinity site that overlaps with the antibiotic binding pocket. The binding of CoASH to the high-affinity site occurs with a small, unfavorable enthalpy and a favorable entropy. Binding to the second site is highly exothermic and is accompanied by an unfavorable entropic contribution. The presence of an aminoglycoside alters the binding of CoASH to AAC dramatically such that the binding occurs with a favorable enthalpy ($\Delta H < 0$) and an unfavorable entropy ($T\Delta S < 0$). This is irrespective of which aminoglycoside is the cosubstrate and occurs without a significant change in the affinity of CoASH for AAC. Also, antibiotics eliminate binding of CoASH to the second site. These data allowed the enthalpies of all six equilibria present in a ternary system (AAC−antibiotic−coenzyme) to be determined for the first time for an aminoglycoside-modifying enzyme. NMR experiments also shed light on the dynamic nature of AAC as fast, slow, and intermediary exchanges between apoenzyme- and coenzyme-bound forms were observed.

Aminoglycoside (AG)[1] antibiotics comprise a group of clinically used drugs that are experiencing an ongoing loss of their ability to fight bacterial infections because of evolving bacterial resistance to them. While several resistance mechanisms have been observed, the most prominent is the enzymatic covalent modification of the antibiotic. More than 40 enzymes that are responsible for aminoglycoside modification from both Gram-positive and Gram-negative bacteria have been isolated. The enzymes have been divided into three categories on the basis of the chemical group transferred and include phosphotransferases, nucleotidyltransferases, and acetyltransferases. The result of such modifications to an aminoglycoside is a significant decrease in the affinity for the ribosomal target of the antibiotic; hence, protein translation can occur normally in the bacterium (*1*, *2*).

Although a large number of crystal structures of aminoglycoside-modifying enzymes (AGMEs) that catalyze acetylation, nucleotidylation, or phosphorylation of aminoglycosides are available (*3*−*9*), thermodynamic studies of these enzymes are quite limited (*10*−*15*). Furthermore, there are no data available for an enzyme that modifies the central 2-deoxystreptamine (2-DOS) ring of aminoglycoside antibiotics (*10*−*14*, *16*). We have presented the kinetic and thermodynamic properties of the aminoglycoside acetyltransferase (3)-IIIb (AAC) and its interactions with antibiotic substrates in the preceding paper (DOI 10.1021/bi100155j). In this paper, we describe the thermodynamic and kinetic properties of AAC−coenzyme complexes determined by a variety of biophysical methods, including ITC, fluorescence, and NMR. Because AAC does not require metals for efficient binding and catalysis of substrates, as observed with the nucleotide-utilizing enzymes, these data provide the complementary information necessary to thermodynamically quantify all six equilibria associated with the AAC−coenzyme−antibiotic ternary system (*17*, *18*). This is the first such analysis for any aminoglycoside-modifying enzyme. Moreover, these data complete the first kinetic and thermodynamic characterization of an enzyme that modifies the common 2-deoxystreptamine ring of aminoglycosides.

EXPERIMENTAL PROCEDURES

Chemicals and Reagents. Ion exchange matrix (Macro Q) was purchased from Bio-Rad Laboratories (Hercules, CA), while high-performance Ni-Sepharose resin was purchased from Amersham Biosciences (Piscataway, NJ). IPTG was obtained

[†]This work is supported by a grant from the National Science Foundation (MCB-0842743 to E.H.S.) and by the Hunsicker Award (to E.H.S.) through the Department of Biochemistry Cellular and Molecular Biology at The University of Tennessee. A.L.N. is partly supported by the Department of Energy EPSCoR Implementation award (DE-FG02-08ER46528).

*To whom correspondence should be addressed: Walters Life Sciences Bldg. M407, The University of Tennessee, Knoxville, TN 37996-0840. Telephone: (865) 974-2668. Fax: (865) 974-6306. E-mail: serpersu@utk.edu.

[1]Abbreviations: AG, aminoglycoside; AGME, aminoglycoside-modifying enzyme; 2-DOS, 2-deoxystreptamine; IPTG, isopropyl β-D-1-thiogalactopyranoside; Tris-HCl, 2-amino-2-(hydroxymethyl)propane-1,3-diol hydrochloride; PIPES, piperazine-1,4-bis(2-ethanesulfonic acid); HEPES, 4-(2-hydroxyethyl)-1-piperazineethanesulfonic acid; AcCoA, acetyl coenzyme A; CoASH, coenzyme A; ITC, isothermal titration calorimetry; NMR, nuclear magnetic resonance; HSQC, heteronuclear single-quantum coherence.

 Published on Web 04/13/2010

from Inalco Spa (Milan, Italy), and purified thrombin was graciously provided by E. Fernandez (The University of Tennessee). All other aminoglycosides, coenzymes, and reagents were purchased at the highest possible purity from Sigma.

Overexpression and Purification of AAC. AAC, recovered from inclusion bodies and used in previous work (*19*), was recloned with a six-His tag and overexpressed in *Escherichia coli* BL21(DE3) cells in a soluble form. Purification and removal of the His tag were performed as described in the preceding paper (DOI 10.1021/bi100155j). Briefly, cells were serially grown to 4 L in Luria broth and induced for 4 h with IPTG prior to being harvested and stored at −80 °C. Purification of the six-His tag AAC was performed with a Ni-Sepharose affinity resin and the His tag subsequently cleaved. Free His tag and thrombin used for tag cleavage were separated from AAC by nickel affinity and anion exchange chromatography, respectively.

Fluorescence Spectroscopy. The change in intrinsic tryptophan fluorescence intensity was used to detect AAC−coenzyme A (CoASH) interactions. A Perkin-Elmer (Boston, MA) model LS 55 fluorescence spectrometer equipped with a stirred four-position cell changer with a 1 cm light path was used. The excitation wavelength was 295 nm for tryptophan selection, while emission was measured at 345 nm. Sample solutions contained 1 μM AAC, 100 mM NaCl, and 50 mM Tris-HCl (pH 7.6) at 25 °C; 1−5 μL of concentrated, serially diluted CoASH stocks were titrated into a sample volume of 2.5 mL. The maximum sample dilution was 2.4%. To obtain dissociation constants (K_D), the percent change in fluorescence intensity was plotted versus substrate concentration and saturation curves were fit to the single-site binding equation:

$$(\Delta F/F_0) \times 100 = [(\Delta F/F_0) \times 100][S]/(K_D + [S]) \quad (1)$$

where $(\Delta F/F_0) \times 100$ is the percent change in fluorescence intensity and F_0 represents the fluorescence intensity of the sample prior to the addition of substrate. Titrations of the coenzyme yielded an increase in fluorescence intensity, while identical additions to buffer alone showed no change in the fluorescence signals.

Isothermal Titration Calorimetry (ITC). ITC experiments were performed on a VP-ITC microcalorimeter from Microcal, Inc. (Northampton, MA), at 25 °C. AAC concentrations were between 10 and 20 μM to maintain c values ([binding sites] × association constant) within the range of 1−100 for greater accuracy of association constant (K_A) measurements. CoASH was diluted into the final dialysis buffer used in enzyme purification and was present in the syringe at concentrations 20−40 times greater than that of AAC in the cell. Both cell and syringe solutions contained 100 mM NaCl and the appropriate buffer at 50 mM (pH 7.6) at 25 °C. In ternary experiments, the antibiotic was included in the cell solution at a saturating concentration while CoASH was titrated from the syringe. Samples were degassed for 10 min prior to being loaded. Titrations of ligands into buffer were performed as a control, and the resulting heats of ligand dilution were subtracted from the experimental data prior to curve fitting. Both pH and activity were monitored before and after each experiment. In all cases, the enzymatic activity remained greater than 87% of the starting activity and the pH unaltered at the end of titrations. Thermograms were integrated using Origin software provided by the instrument manufacturer. Formation of the binary enzyme−CoASH complex was fit to a sequential binding model. For ternary complexes, the best fits were obtained with one-site binding. Since binding of ligands to the enzyme causes shifts in the pK_a values of several functional groups, all titrations were performed individually in Tris-HCl, HEPES, and PIPES buffers with heats of ionization (ΔH_{ion}) of 11.4, 5.02, and 2.74 kcal/mol, respectively, to determine the intrinsic enthalpy as described previously (*10*, *12*, *14*, *20*). ΔG values were calculated from association constants (K_A) derived from fitted titration curves using the equation $\Delta G = -RT \ln(K_A)$. $T\Delta S$ values were then determined from the relationship $\Delta G = \Delta H_{int} - T\Delta S$.

Binding of aminoglycoside to CoASH was also assessed via ITC. Here, 50× antibiotic was titrated into CoASH in the cell at 800 μM. Both cell and syringe solutions contained the appropriate buffer at 50 mM (pH 7.6) at 25 °C and 100 mM NaCl.

Steady State Kinetics. To obtain steady state kinetic information, a Cary-Win UV−vis spectrophotometer (Varian, Palo Alto, CA) was used to monitor AAC activity via a continuous assay. This assay uses a coupled chemical reaction in which an increase in the absorbance of pyridine-4-thiolate at 324 nm indicates turnover as described previously (*19*, *21*). Samples consisted of 100 mM NaCl and 50 mM Tris-HCl (pH 7.6) at 25 °C. AAC (10 nM) was used in each assay, and the reaction was initiated by addition of aminoglycoside to a final concentration of 100 μM. Reactions followed Michaelis−Menten type kinetics with all substrates tested. Reported kinetic parameters were determined via fits of specific activity (micromoles per minute per milligram) versus coenzyme concentration to the Michaelis−Menten equation. Turnover rates (k_{cat}) were calculated from the relationship $V_{max} = k_{cat}[E]_T$.

Nuclear Magnetic Resonance. Nuclear magnetic resonance (NMR) spectroscopy experiments were performed using a 600 MHz, Varian Inova spectrometer equipped with a ^{2}H, ^{13}C, ^{15}N triple-resonance cryogenic probe at The University of Tennessee; 230 μM uniformly ^{15}N-labeled AAC in 100 mM NaCl and 50 mM Tris-HCl (pH 7.6) at 25 °C was titrated with 1−3 μL increments from concentrated stocks of CoASH. Sensitivity-enhanced ^{1}H−^{15}N HSQC (heteronuclear single-quantum coherence) correlation spectra (*22*) were recorded with 64−128 scans of 64 increments in the ^{15}N dimension with the *TROSY* (*23*) option and a delay of 1.5 s between scans; 2048 data points were collected with an acquisition time of 128 ms. Data were processed with NMRpipe (*24*). FID was multiplied with a sin^2 window function in the acquisition dimension before Fourier transformation. No baseline correction or other cosmetic procedures were applied. Spectra were exported to Sparky (T. D. Goddard and D. G. Kneller, SPARKY 3, University of California, San Francisco) for analysis and display.

RESULTS AND DISCUSSION

Kinetic Selectivity of the Coenzyme. Steady state kinetic analysis reveals that several coenzyme molecules can serve as substrates, with acetyl coenzyme A (AcCoA) being the most preferred. The K_m of AcCoA is ∼17 μM and is irrespective of which antibiotic is present as the cosubstrate (Table 1). Propionyl CoA and malonyl CoA were both found to be catalytically utilized, albeit with K_m values 4−10-fold larger than that of AcCoA and specificity constants 1.5−2 orders of magnitude lower. For all parameters, malonyl CoA was the least favored. This is similar to AAC(6′)-Iy (*16*) and suggests that bulky substitutions at the reactive sulfur hinder coenzyme binding and/or distort the alignment of the bound ligand, causing a decrease in the reaction rate relative to that of acetyl CoA.

Table 1: Kinetic Parameters for Coenzymes

substrate[a]	K_m (μM)	V_{max} (μmol min^{-1} mg^{-1})	k_{cat} (s^{-1})	k_{cat}/K_m ($\times 10^6$ M^{-1} s^{-1})
AcCoA (K)	15.4 ± 0.4	76.2 ± 0.9	39.4 ± 0.4	2.6 ± 0.1
AcCoA (N)	17.0 ± 2.1	20.3 ± 0.2	10.5 ± 0.1	0.6 ± 0.1
n-propionyl CoA (K)[b]	88.6 ± 20.5	19.8 ± 1.4	10.2 ± 0.7	0.12 ± 0.03
malonyl CoA (K)[b]	234 ± 62	11.1 ± 1.1	5.7 ± 0.5	0.03 ± 0.01

[a]K and N parenthetical notations denote kanamycin A and neomycin B, respectively, as the antibiotic held constant in the experiment. [b]Data and errors for *n*-propionyl CoA and malonyl CoA are from curve fitting of Michaelis−Menten plots. All others were calculated from the average of two trials, with the errors being the standard error of the mean.

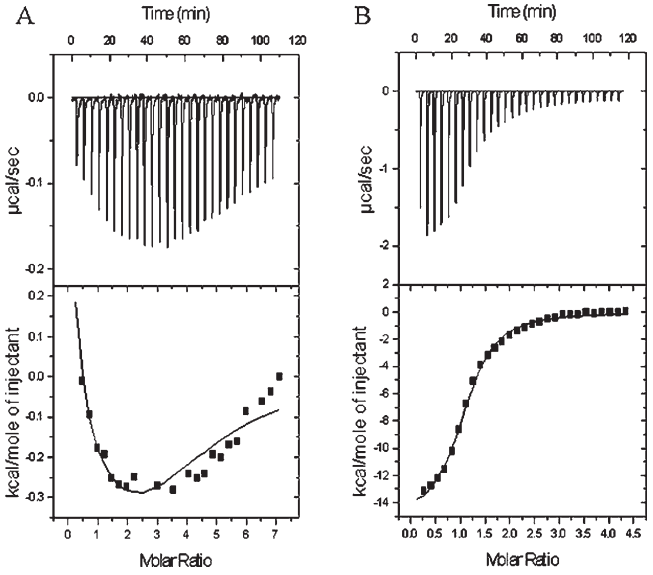

FIGURE 1: Binding of coenzyme A to AAC as detected by ITC. Thermograms (top) representing the titration of AAC with CoASH are shown with fitted data in isotherms (bottom). Lines represent fits to data as described in the text. (A) The biphasic nature of CoASH binding to AAC alone demonstrates a two-site interaction. (B) CoASH titrated into an AAC−antibiotic complex yields a monophasic curve with a much greater heat signal.

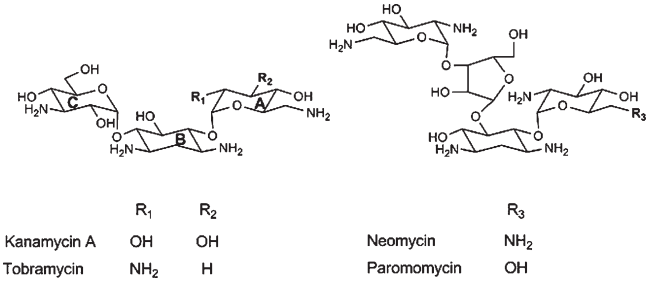

FIGURE 2: Aminoglycoside structures. The 2-deoxystreptamine ring (ring B) is 4,6-disubstituted in the kanamycin class (left), while neomycin class (right) aminoglycosides are 4,5-disubstituted.

Coenzyme A Binding. Unlike that of aminoglycosides, binding of CoASH to AAC shows a biphasic pattern in which endothermic, high-affinity binding to the first site is followed by low-affinity, exothermic binding to a second site (Figure 1A). In the experiment shown in Figure 1A, data fit to a two-site sequential binding equation which produced a 1 order of magnitude difference in affinity. Because of the high error of this fit and nonsaturation of the second site, we performed a second experiment in which the first site was saturated with CoASH prior to titration of more CoASH to yield a reliable, saturated curve for deriving second-site thermodynamic parameters. In this experiment (conducted in two individual buffers), data fit best to a single-site model with a stoichiometry of 2.9 ± 0.2, indicating a secondary, less specific interaction in which the K_D is 48.2 ± 1.2 μM, ΔH_{int} is −3.7 ± 0.1, and $T\Delta S$ is 9.6 ± 0.3, hence making ΔG equal −5.9 ± 0.2 kcal/mol (Figure S2 of the Supporting Information). These values were consistent with the trend observed in the higher-error, sequential fit for the second site aforementioned. Attempts to selectively saturate the first site by limiting the concentration of CoASH in the titration syringe were unsuccessful due to the small amount of heat associated with this interaction, even in the presence of a high AAC concentration. However, interaction of CoASH with AAC was also monitored via intrinsic tryptophan fluorescence and NMR spectroscopy (see the discussion below). In both cases, >90% saturation of the first site was determined to occur at an enzyme:ligand ratio of ~3:1. With this information, the data points in the experiment of Figure 1A higher than 3:1 were eliminated, thus allowing analysis of only the first site. These data fit to a single-site model in which the stoichiometry was 0.91 ± 0.08, with a K_D of 1.9 ± 1.2 μM, a ΔH_{obs} of 0.4 ± 0.1, a $T\Delta S$ of 8.2 ± 2.1, and a ΔG of −7.8 ± 2.0 kcal/mol. The dissociation constant determined in this manner agreed well with those determined by fluorescence and NMR. We also calculated the expected heat of first-site CoASH interaction from independent experiments and confirmed the low heat experimentally observed (discussed in the next section). At this point, we emphasize that the reproducible observation of two distinct binding modes itself is more important than the absolute values associated with them. Two thermodynamically distinct modes of CoASH binding were also observed with phosphopantetheine adenylyltransferase (*25*); thus, ours is not an orphan phenomenon.

In the presence of aminoglycosides (Figure 2), the thermograms are dramatically altered (Figure 1) and binding of CoASH to AAC becomes highly exothermic without a significant change in the dissociation constant of the high-affinity site. In individual experiments, six different aminoglycosides were added to AAC at a saturating level as the cosubstrate. Titration of CoASH into AAC−aminoglycoside complexes yields K_D values that range between 2.0 and 3.6 μM, excluding the weaker binding kanamycin A (Table 2). Enthalpy, entropy, and free energy values are also independent of the antibiotic, where ΔH_{int} ranges from −16.7 to −20.8 kcal/mol, $T\Delta S$ from −9.0 to −11.9 kcal/mol (excluding kanamycin A), and ΔG from −7.1 to −7.8 kcal/mol (Table 2). There is no indication of binding to a second site as all stoichiometries to the enzyme are 1/1 mol/mol and the best fits to the data are obtained with a single-site binding model regardless of the aminoglycoside present. These observations suggest that the secondary CoASH interacts with the aminoglycoside site with a low affinity that is eliminated by the presence of aminoglycoside. This coincides well with the homology model [discussed in

Table 2: Thermodynamic Parameters for Coenzyme A Binding to AAC−Antibiotic Complexes[a]

cosubstrate	N	K_D (μM)	ΔH_{int} (kcal/mol)	$-T\Delta S$ (kcal/mol)	ΔG (kcal/mol)	Δn
neomycin B	1.2 ± 0.1	3.6 ± 1.4	−17.0 ± 3.2	9.5 ± 1.8	−7.5 ± 0.3	0.6 ± 0.1
paromomycin	1.0 ± 0.02	2.6 ± 1.1	−18.6 ± 0.2	10.9 ± 0.1	−7.7 ± 0.3	1.2 ± 0.02
ribostamycin	1.3 ± 0.1	2.5 ± 0.3	−19.0 ± 0.8	11.3 ± 0.5	−7.7 ± 0.1	0.7 ± 0.02
kanamycin A	1.1 ± 0.1	6.6 ± 1.5	−20.8 ± 1.6	13.6 ± 1.1	−7.1 ± 0.1	1.4 ± 0.3
kanamycin B	1.1 ± 0.1	2.0 ± 0.5	−19.8 ± 0.1	11.9 ± 0.2	−7.8 ± 0.1	0.8 ± 0.1
tobramycin	1.2 ± 0.1	2.5 ± 0.7	−16.7 ± 0.2	9.0 ± 0.2	−7.7 ± 0.1	0.6 ± 0.01

[a]Given errors are calculated as the standard error of the mean of two to six trials. Errors in the intrinsic enthalpy (ΔH_{int}) and the net protonation (Δn) were derived from the deviation from linearity of ΔH_{obs} vs ΔH_{ion} curves (Figure 6).

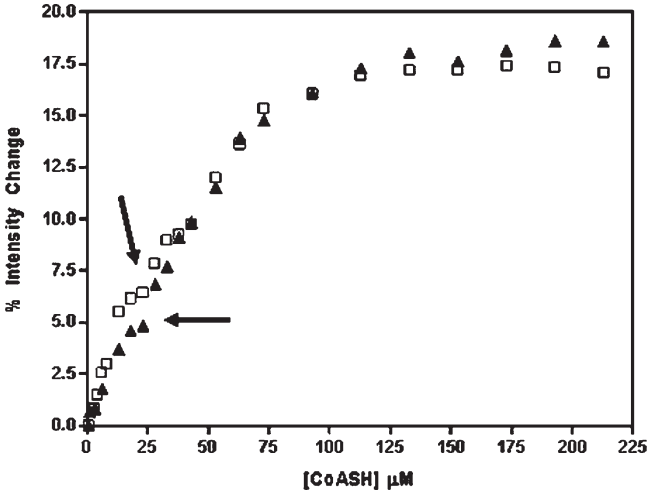

FIGURE 3: Fluorescence titration of CoASH into AAC. Change in intrinsic fluorescence intensity as a function of CoASH added to AAC. The biphasic nature is more subtle here than in ITC but was reproduced in three separate trials. For the sake of clarity, only two are shown with triangles and empty squares, with arrows illustrating the transition points.

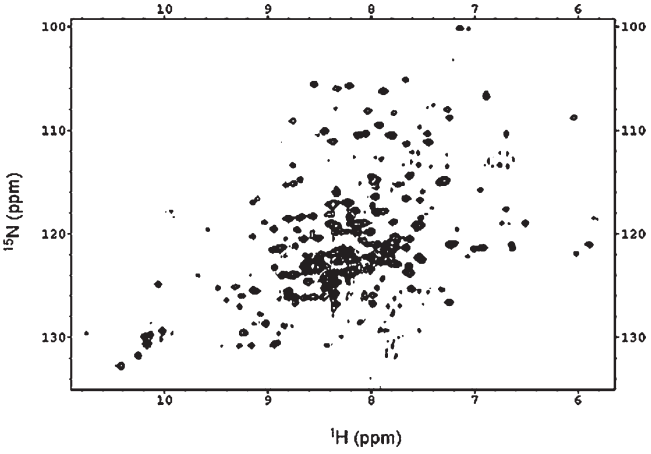

FIGURE 4: $^1H-^{15}N$ HSQC correlation spectrum of 230 μM apo-AAC in Tris-HCl (pH 7.6) at 25 °C. Sixty-four scans with 2048 data points were acquired.

the preceding paper (DOI 10.1021/bi100155j)] in which several lysine and arginine residues are in the vicinity of the putative antibiotic pocket. This could serve as a basis for the secondary coenzyme molecule interaction as CoASH contains three highly negative phosphate moieties.

Initial fluorescence experiments also revealed a biphasic curve for titration of CoASH into AAC, albeit the transition is more subtle than in ITC (Figure 3). Nevertheless, multiple trials reproduced identical results and increased confidence that the transition was indeed real. To more accurately determine dissociation constants, the experiments were repeated with more points placed in the lower CoASH concentration range (data not shown). These trials showed that the signal intensity change for selectively binding to the first site is small (4−6%) and yields a K_D of 3.8 ± 1.3 μM. For the second site, the dissociation constant is 47.8 ± 2.5 μM and has an intensity increase of 12−15%. No further change is observed in fluorescence intensity upon addition of antibiotics to AAC when the CoASH concentration is sufficiently high to saturate both sites. In conjunction with ITC, these data also suggest that a second coenzyme molecule may interact with the antibiotic binding site where the tryptophan signals are altered to an extent similar to that of the antibiotic. Indeed, addition of an elevated CoASH concentration to the apoenzyme invoked a large intensity change similar to that observed for antibiotic alone [preceding paper (DOI 10.1021/bi100155j)]. The AAC homology model [also in the preceding paper (DOI 10.1021/bi100155j)] supports these findings in that the closest tryptophan to the coenzyme site is 11.4 Å distant and is the same one that is positioned directly in the antibiotic pocket. Thus, it is expected that the coenzyme, being farther from this residue, can induce only small changes in fluorescence intensity while the antibiotic creates large changes.

A series of $^1H-^{15}N$ heteronuclear single-quantum correlation (HSQC) NMR spectra provide structural support for the two-site coenzyme model in which two distinct sets of spectral changes were observed upon CoASH titration. These spectra yielded >200 observable peaks for this 29 kDa protein (Figure 4). Incremental addition of CoASH to ^{15}N-enriched AAC causes a small number of peaks (~20) to shift until the first CoASH binding site is saturated (Figure 5). A dissociation constant of 1.5 ± 0.5 μM was determined for the binding of CoASH to AAC to this site. Upon further titration, several different peaks appear in the spectrum and increase in intensity to the saturation of the second site but do not shift. These experiments reveal interesting dynamic properties of AAC. First, during saturation of the first site, several peaks show a steady shift without broadening, indicating these amides are in fast exchange between the ligand-bound and apo forms of the enzyme (resonance 3 of Figure 5). Several other peaks, on the other hand, show that they are in slow exchange as judged by the intensity of the peaks for the apoenzyme and ligand-bound enzyme being proportional to the saturation level. Finally, further addition of CoASH beyond the saturation of the high-affinity site caused some additional peaks to appear in the spectrum, indicating that these amides were in an intermediary exchange regime in both apo-AAC and the AAC−CoASH complex and became visible only when the

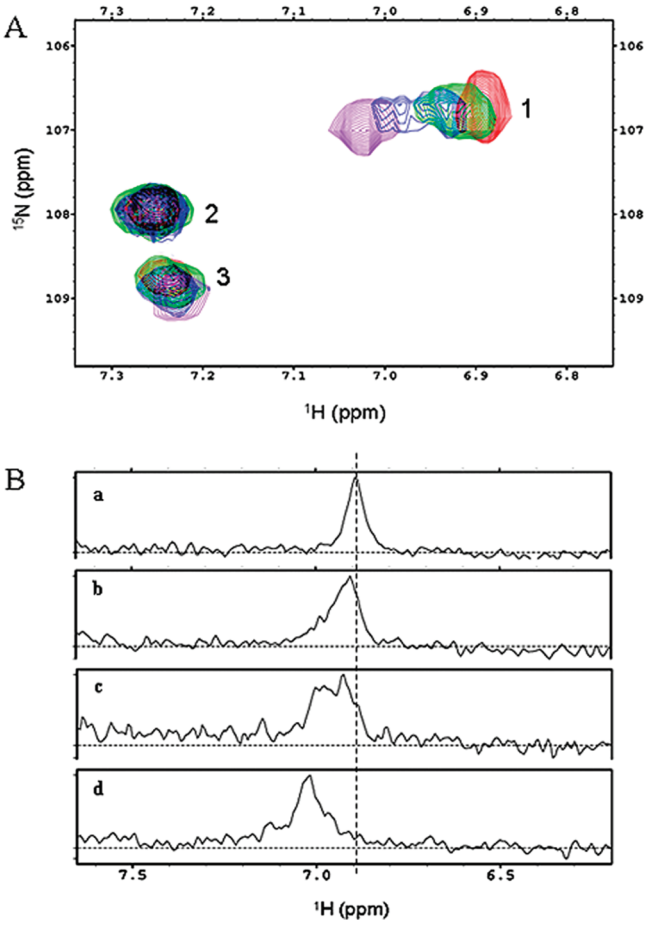

FIGURE 5: NMR detection of binding of CoASH to AAC. (A) An expanded region of the ^{1}H−^{15}N HSQC spectrum of AAC in which three resonances demonstrate different behavior in response to CoASH binding. Peak positions for 230 μM apo-AAC and 160, 320, and 960 μM CoASH additions are shown in overlaid spectra colored red, green, blue, and purple, respectively. (B) The ^{1}H spectrum of peak 1 from panel A demonstrates the slow (or borderline between slow and intermediary) exchange of this backbone amide between the free and CoASH-bound conformations: apo-AAC (a) and 160 (b), 320 (c), and 960 μM CoASH (d). The vertical dashed line is given for a positional reference.

second CoASH binding site was occupied. These observations clearly demonstrate the highly dynamic nature of AAC and show that all three exchange regimes (fast, intermediary, and slow) can be observed with one bound ligand. This behavior may be the key for the substrate promiscuity of AAC. In this respect, AAC is like APH (3′)-IIIa, which also has a very broad substrate specificity and is an unusually flexible molecule in solution such that the apo form of this 31 kDa enzyme can exchange all of the amide protons in solution (*26*). Thus, the flexibility of AGMEs may be a general property and the main cause of their substrate promiscuity.

Overall, ITC, NMR, and fluorescence yield similar results, although dissociation constants vary slightly depending on the method of measurement for the complexes of CoASH with the enzyme in the absence and presence of aminoglycosides. These discrepancies are most likely due to the use of a wide range of enzyme concentrations, which covered a span of 2 orders of magnitude, required for each technique as described in Experimental Procedures.

Thermodynamic Analysis of a Ternary System. The thermodynamics of a ternary system (enzyme + ligand1 + ligand2) are described by six equilibria (*17*) (Figure S1 of the Supporting Information). For the first time for any aminoglycoside-modifying enzyme, this work has allowed us to determine thermodynamic parameters of all relevant complexes. Since enthalpy is a state property, one can calculate the overall heat of formation of the ternary complex, AAC−CoASH−NeoB, from different pathways as shown below:

Pathway 1

$$\begin{array}{l} \mathrm{AAC + NeoB \leftrightarrow AAC-NeoB} \\ + \\ \mathrm{AAC-NeoB + CoASH \leftrightarrow AAC-NeoB-CoASH} \\ \hline \mathrm{AAC + NeoB + CoASH \leftrightarrow AAC-NeoB-CoASH} \end{array}$$

$$\begin{array}{rcl} \Delta H_1 & = & -8.3 \pm 0.4 \text{ kcal/mol} \\ + & & \\ \Delta H_2 & = & -10.5 \pm 0.1 \text{ kcal/mol} \\ \hline \Delta H_3 & = & -18.8 \pm 0.9 \text{ kcal/mol} \end{array}$$

Pathway 2.

$$\begin{array}{l} \mathrm{AAC + CoASH \leftrightarrow AAC-CoASH} \\ + \\ \mathrm{AAC-CoASH + NeoB \leftrightarrow AAC-NeoB-CoASH} \\ \hline \mathrm{AAC + NeoB + CoASH \leftrightarrow AAC-NeoB-CoASH} \end{array}$$

$$\begin{array}{rcl} \Delta H_4 & = & 0.4 \pm 0.1 \text{ kcal/mol} \\ + & & \\ \Delta H_5 & = & -18.6 \pm 0.2 \text{ kcal/mol} \\ \hline \Delta H_6 & = & -18.2 \pm 2.4 \text{ kcal/mol} \end{array}$$

ΔH_3 and ΔH_6 are identical within error and are calculated from individual, independent experiments. Thus, it is reasonable to conclude that the average of these numbers (−18.5 kcal/mol) represents the heat of formation of the AAC−NeoB−coenzyme complex. Applying this rationale to the other aminoglycosides, one calculates the overall heat of formation for the ternary system as -9.7 ± 0.7, -14.4 ± 0.2, -8.8 ± 0.8, -10.7 ± 1.0, and -5.3 ± 2.1 kcal/mol for paromomycin, ribostamycin, kanamycin B, tobramycin, and kanamycin A, respectively. These values are averages of ΔH_3 and ΔH_6 for each aminoglycoside, with errors being the deviation of each of these enthalpies from the average.

In these calculations, we used ΔH_{obs}, instead of ΔH_{int}, determined in the same buffer for all complexes because ΔH_{int} for the binary AAC−CoASH complex could not be determined experimentally. This was due to the fact that the enthalpy of binding of CoASH to the high-affinity site is very low and easily masked by the large enthalpy of binding to the second site in experiments performed with several different buffers. The small heat of interaction can be validated by utilizing the additive property of thermodynamic parameters as described above. Consider the following equilibria and their experimentally determined enthalpies using neomycin B as the aminoglycoside substrate.

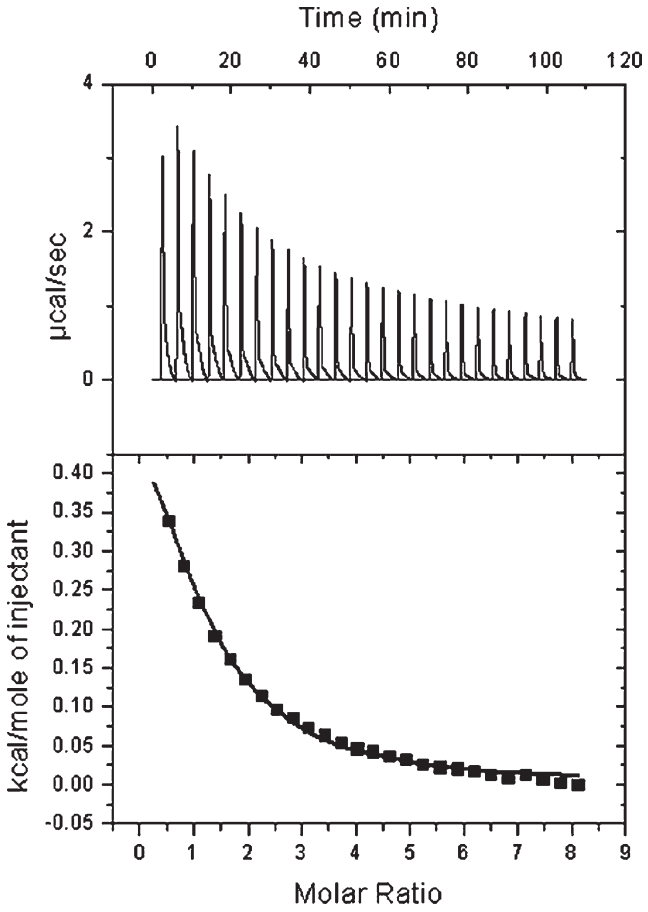

FIGURE 6: Formation of the CoASH−neomycin complex. Titration of neomycin into a solution of CoASH yields a saturable curve with an endothermic heat signature as detected by ITC. The thermogram (top) and isotherm (bottom) are shown. Data fit to a single-site binding model, as described in Experimental Procedures, are shown as a solid line in the isotherm.

$$\begin{aligned}&\text{AAC}-\text{NeoB}-\text{CoASH}\leftrightarrow\text{AAC}-\text{NeoB}+\text{CoASH}\\&+\\&\text{AAC}-\text{CoASH}+\text{NeoB}\leftrightarrow\text{AAC}-\text{NeoB}-\text{CoASH}\\&+\\&\text{AAC}-\text{NeoB}\leftrightarrow\text{AAC}+\text{NeoB}\\&\text{---------------------------------------}\\&\text{AAC}-\text{CoASH}\leftrightarrow\text{AAC}+\text{CoASH}\end{aligned}$$

$$\begin{aligned}\Delta H_2 &= 10.5\pm0.1\ \text{kcal/mol}\\&+\\\Delta H_5 &= -18.6\pm0.2\ \text{kcal/mol}\\&+\\\Delta H_1 &= 8.3\pm0.4\ \text{kcal/mol}\\&\text{----------------------}\\\Delta H_{4(\text{calc})} &= 0.2\pm0.1\ \text{kcal/mol}\end{aligned}$$

This calculated value is virtually within error of the experimentally determined one and demonstrates that the heat contribution from the interaction of CoASH with AAC will be small. Similar analyses with different antibiotics yield heats of dissociation between −0.7 and 1.7 kcal/mol, with the exception of that of kanamycin A.

Using the same thermodynamic relationship as described above with ΔH_{int} values listed in Table 2 to calculate a theoretical ΔH_{int} for the formation of the binary AAC−CoASH complex, a range of values between −1.9 and −5.3 kcal/mol (average of −3.7 ± 0.7 kcal/mol) were obtained when data for neomycin, paromomycin, kanamycin B, and tobramycin were used separately (the two weakest binding aminoglycosides, ribostamycin and kanamycin A, were omitted). These values are also close to those determined in a single buffer (ΔH_{obs}) and indicate that there is a small contribution of the heat of ionization due to small shifts in pK_a values of functional groups. It should also be noted that CoASH and not AcCoA was used in all experiments to prevent catalysis but that AcCoA binary titrations yielded results similar to those of CoASH.[2]

Another experimentally unattainable heat of binding representing the binding of the binary CoASH−AG complex to AAC was calculated by using the experimentally determined enthalpy for the formation of the CoASH−NeoB complex (Figure 6) with the calculated overall enthalpy for the ternary AAC−CoASH−NeoB complex as shown below.

$$\begin{aligned}&\text{AAC}+\text{CoASH}+\text{NeoB}\leftrightarrow\text{AAC}-\text{CoASH}-\text{NeoB}\\&+\\&\text{NeoB}-\text{CoASH}\leftrightarrow\text{NeoB}+\text{CoASH}\\&\text{---------------------------------------}\\&\text{AAC}+\text{NeoB}-\text{CoASH}\leftrightarrow\text{AAC}-\text{NeoB}-\text{CoASH}\end{aligned}$$

$$\begin{aligned}\Delta H_3 &= -18.8\pm0.4\ \text{kcal/mol}\\&+\\\Delta H_8 &= -0.8\pm0.1\ \text{kcal/mol}\\&\text{----------------------}\\\Delta H_7 &= -19.6\pm2.3\ \text{kcal/mol}\end{aligned}$$

Thus, the enthalpies of the formation of all complexes involved in the ternary system of the enzyme and both ligands (CoASH and aminoglycosides) are determined.

CONCLUSIONS

This work represents the characterization of an aminoglycoside acetyltransferase enzyme and its interactions with coenzymes. Here we have shown that AcCoA is the preferred substrate where its affinity is irrespective of which aminoglycoside is present as the cosubstrate. Both malonyl and propionyl CoA can also provide catalysis, although the affinities and turnover rates are significantly weaker than those of AcCoA.

ITC, fluorescence, and NMR studies showed that the coenzyme binds to both a high-affinity site and a low-affinity site, the latter of which interferes with aminoglycoside interaction as the presence of the antibiotic reduces the stoichiometry from ≥2 to a perfect 1:1 molar ratio. Furthermore, binding to the first site is associated with a low heat signature. In the presence of an antibiotic, however, the heat of interaction of CoASH increases significantly without a significant change in the affinity for the first site, and all thermodynamic parameters (K_D, ΔH_{int}, $T\Delta S$, and ΔG) are irrespective of the antibiotic cosubstrate.

To the best of our knowledge, this paper also presents the first calculation of the heat of formation of all six complexes involved in a ternary system. Experimental data from two separate pathways for the formation of the ternary complex confirm each other and allow determination of enthalpies that cannot be accessed by experimental means. All aminoglycosides tested, with the exception of the weakly binding kanamycin A, also confirmed the data in an aminoglycoside-independent manner.

[2]A. L. Norris and E. H. Serpersu, unpublished data, 2009.

NMR studies showed that coenzyme A binding invokes all three exchange regimes between apo and ligand-bound forms of AAC. This demonstrates the dynamic nature of the protein and implies that flexibility may be the common denominator for the highly promiscuous AGMEs. AAC has one of the broadest substrate profiles among AGMEs and acetylates an important site common to all aminoglycosides. Therefore, understanding its thermodynamic properties is crucial in drug design efforts to overcome bacterial resistance to antibiotics.

SUPPORTING INFORMATION AVAILABLE

Thermodynamic cycle illustrating the six equilibria involved in a ternary system (Figure S1) and ITC data for the selective saturation of the secondary CoASH site (Figure S2). This material is available free of charge via the Internet at http://pubs.acs.org.

REFERENCES

1. Spotts, C. R., and Stanier, R. Y. (1961) Mechanism of Streptomycin Action on Bacteria: Unitary Hypothesis. *Nature 192*, 633–637.
2. Moazed, D., and Noller, H. F. (1987) Interaction of Antibiotics with Functional Sites in 16s Ribosomal-RNA. *Nature 327*, 389–394.
3. Fong, D. H., and Berghuis, A. M. (2002) Substrate promiscuity of an aminoglycoside antibiotic resistance enzyme via target mimicry. *EMBO J. 21*, 2323–2331.
4. Nurizzo, D., Shewry, S. C., Perlin, M. H., Brown, S. A., Dholakia, J. N., Fuchs, R. L., Deva, T., Baker, E. N., and Smith, C. A. (2003) The crystal structure of aminoglycoside-3′-phosphotransferase-IIa, an enzyme responsible for antibiotic resistance. *J. Mol. Biol. 327*, 491–506.
5. Pedersen, L. C., Benning, M. M., and Holden, H. M. (1995) Structural Investigation of the Antibiotic and ATP-Binding Sites in Kanamycin Nucleotidyltransferase. *Biochemistry 34*, 13305–13311.
6. Vetting, M. W., Hegde, S. S., Javid-Majd, F., Blanchard, J. S., and Roderick, S. L. (2002) Aminoglycoside 2′-N-acetyltransferase from *Mycobacterium tuberculosis* in complex with coenzyme A and aminoglycoside substrates. *Nat. Struct. Biol. 9*, 653–658.
7. Wolf, E., Vassilev, A., Makino, Y., Sali, A., Nakatani, Y., and Burley, S. K. (1998) Crystal structure of a GCN5-related *N*-acetyltransferase: *Serratia marcescens* aminoglycoside 3-*N*-acetyltransferase. *Cell 94*, 439–449.
8. Wybenga-Groot, L. E., Draker, K., Wright, G. D., and Berghuis, A. M. (1999) Crystal structure of an aminoglycoside 6′-N-acetyltransferase: Defining the GCN5-related N-acetyltransferase superfamily fold. *Struct. Folding Des. 7*, 497–507.
9. Young, P. G., Walanj, R., Lakshmi, V., Byrnes, L. J., Metcalf, P., Baker, E. N., Vakulenko, S. B., and Smith, C. A. (2009) The Crystal Structures of Substrate and Nucleotide Complexes of *Enterococcus faecium* Aminoglycoside-2″-Phosphotransferase-IIa [APH(2″)-IIa] Provide Insights into Substrate Selectivity in the APH(2″) Subfamily. *J. Bacteriol. 191*, 4133–4143.
10. Ozen, C., Malek, J. M., and Serpersu, E. H. (2006) Dissection of aminoglycoside-enzyme interactions: A calorimetric and NMR study of neomycin B binding to the aminoglycoside phosphotransferase(3′)-IIIa. *J. Am. Chem. Soc. 128*, 15248–15254.
11. Ozen, C., Norris, A. L., Land, M. L., Tjioe, E., and Serpersu, E. H. (2008) Detection of specific solvent rearrangement regions of an enzyme: NMR and ITC studies with aminoglycoside phosphotransferase(3′)-IIIa. *Biochemistry 47*, 40–49.
12. Ozen, C., and Serpersu, E. H. (2004) Thermodynamics of aminoglycoside binding to aminoglycoside-3′-phosphotransferase IIIa studied by isothermal titration calorimetry. *Biochemistry 43*, 14667–14675.
13. Wright, E., and Serpersu, E. H. (2005) Enzyme-Substrate Interactions with an Antibiotic Resistance Enzyme: Aminoglycoside Nucleotidyltransferase(2″)-Ia Characterized by Kinetic and Thermodynamic Methods. *Biochemistry 44*, 11581–11591.
14. Wright, E., and Serpersu, E. H. (2006) Molecular Determinants of Affinity for Aminoglycoside Binding to the Aminoglycoside Nucleotidyltransferase(2″)-Ia. *Biochemistry 45*, 10243–10250.
15. Hegde, S. S., Dam, T. K., Brewer, C. F., and Blanchard, J. S. (2002) Thermodynamics of aminoglycoside and acyl-coenzyme A binding to the *Salmonella enterica* AAC(6′)-Iy aminoglycoside N-acetyltransferase. *Biochemistry 41*, 7519–7527.
16. Hedge, S. S., Dam, T. K., Brewer, C. F., and Blanchard, J. S. (2002) Thermodynamics of aminoglycoside and acyl-coenzyme A binding to the *Salmonella enterica* AAC(6′)-Iy aminoglycoside N-acetyltransferase. *Biochemistry 41*, 7519–7527.
17. Serpersu, E. H., Shortle, D., and Mildvan, A. S. (1986) Kinetic and Magnetic-Resonance Studies of Effects of Genetic Substitution of a Ca^{2+}-Liganding Amino Acid in Staphylococcal Nuclease. *Biochemistry 25*, 68–77.
18. Serpersu, E. H., Shortle, D., and Mildvan, A. S. (1987) Kinetic and magnetic resonance studies of active-site mutants of staphylococcal nuclease: Factors contributing to catalysis. *Biochemistry 26*, 1289–1300.
19. Owston, M. A., and Serpersu, E. H. (2002) Cloning, overexpression, and purification of aminoglycoside antibiotic 3-acetyltransferase-IIIb: Conformational studies with bound substrates. *Biochemistry 41*, 10764–10770.
20. Cox, J. R., and Serpersu, E. H. (1997) Biologically important conformations of aminoglycoside antibiotics bound to an aminoglycoside 3′-phosphotransferase as determined by transferred nuclear Overhauser effect spectroscopy. *Biochemistry 36*, 2353–2359.
21. Williams, J. W., and Northrop, D. B. (1978) Kinetic Mechanisms of Gentamicin Acetyltransferase-I: Antibiotic-Dependent Shift from Rapid to Nonrapid Equilibrium Random Mechanisms. *J. Biol. Chem. 253*, 5902–5907.
22. Bodenhausen, G., and Ruben, D. J. (1980) Natural abundance nitrogen-15 NMR by enhanced heteronuclear spectroscopy. *Chem. Phys. Lett. 69*, 185–188.
23. Salzmann, M., Wider, G., Pervushin, K., and Wutrich, K. (1999) Improved sensitivity and coherence selection for [^{15}N,^{1}H]-TROSY elements in triple resonance experiments. *J. Biomol. NMR 15*, 181–184.
24. Delaglio, F., Grzesiek, S., Vuister, G. W., Zhu, G., Pfeifer, J., and Bax, A. (1995) Nmrpipe: A Multidimensional Spectral Processing System Based on Unix Pipes. *J. Biomol. NMR 6*, 277–293.
25. Miller, J. R., Ohren, J., Sarver, R. W., Mueller, W. T., de Dreu, P., Case, H., and Thanabal, V. (2007) Phosphopantetheine adenylyltransferase from *Escherichia coli*: Investigation of the kinetic mechanism and role in regulation of coenzyme a biosynthesis. *J. Bacteriol. 189*, 8196–8205.
26. Norris, A. L., and Serpersu, E. H. (2009) NMR Detected Hydrogen-Deuterium Exchange Reveals Differential Dynamics of Antibiotic- and Nucleotide-Bound Aminoglycoside Phosphotransferase 3′-IIIa. *J. Am. Chem. Soc. 131*, 8587–8594.